

# Application Report

## CHO-KvLQT1/minK on QPatch

We demonstrate that the CHO-KvLQT1/minK application can be efficiently run on QPatch with high throughput while maintaining high data quality that matches literature values for the given test compounds

### Summary

The human KCNQ1 gene encodes the pore-forming unit of the voltage-gated potassium channel, while KCNE1 encodes for the regulatory minK subunit. The complex is responsible for repolarizing the heart action potential, and in this study we validate that the CHO-KvLQT1/minK application can be efficiently run on QPatch with high throughput, while maintaining high data quality.

### Introduction

The slowly activating, delayed rectifier K<sup>+</sup> channel is among other activities important for regulating the repolarization phase of cardiac action potentials. The KvLQT1/minK channel consists of two transmembrane proteins. Mutations in the genes KCNQ1/KCNE1 coding for KvLQT1/minK are associated with predisposition to deafness, cardiac arrhythmia syndromes including long QT syndrome, atrial fibrillation and sudden infant death syndrome.

Experiments were performed to validate the CHO-KvLQT1/minK cells line on the QPatch. The cell line was characterized in terms of biophysical properties such as IV-relationship, activation, inactivation together with the pharmacological properties of the channel. Furthermore, the current stability and current expression was evaluated. This ion channel is known for having notorious run-down, but by using this QPatch-optimized cell line in combination with the experimental conditions described here, stable current recordings can be obtained.

### Results and discussion

Electrophysiological recordings on KvLQT1/minK channels are often associated with run-down problems. By using the QPatch system and the conditions cited in this report, we overcame the run-down problems.

Figure 1 (top) shows raw traces of KvLQT1/minK with four subsequent additions of extracellular solution measured on a single cell. The corresponding current-time plot data is shown in Figure 1 below.

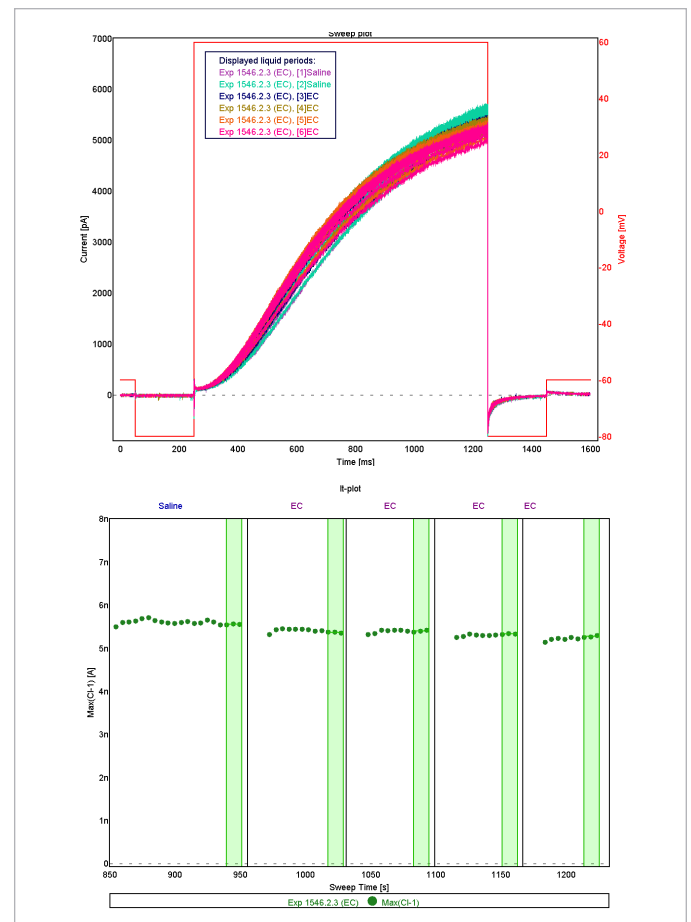
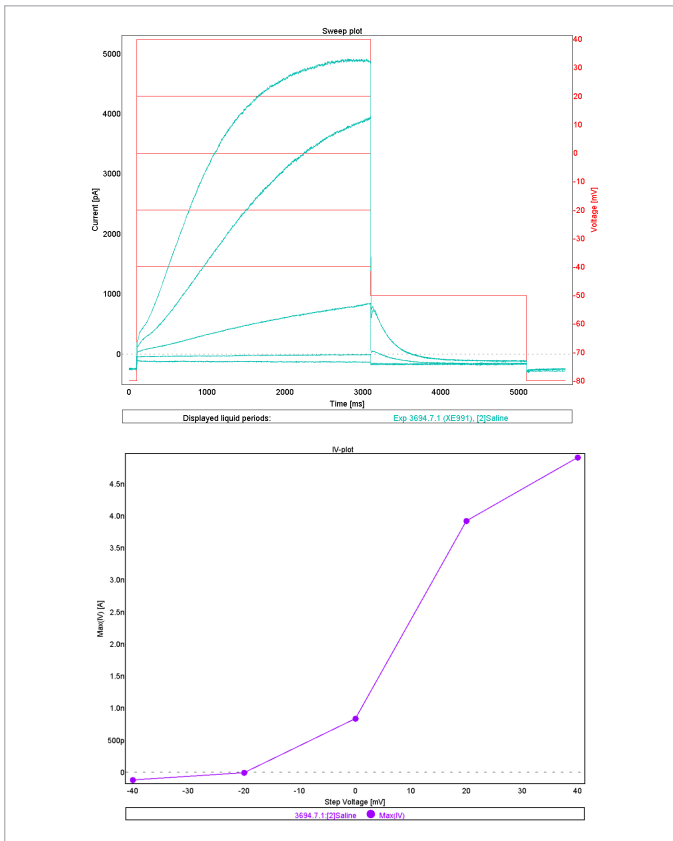


Fig. 1: Raw traces of KvLQT1/minK recordings of 4 consecutive application of extracellular solution on a single cell (top). Bottom: corresponding current-time plot.

Experiments were conducted to evaluate the IV-relationship of the KvLQT1/minK channel. Figure 2 (top) shows the currents elicited at potentials ranging from -80 mV to +40 mV in a representative experiment. The corresponding IV plot is shown in Figure 2 (bottom).



**Fig. 2:** IV-relationship of the KvLQT1/minK channel. Top: Raw data sweeps elicited using an IV-protocol ranging from -80 mV to +40 mV. The voltage step protocol is shown in red. Bottom: corresponding IV-curve measured at the end of the step protocol.

Experiments were performed to evaluate the pharmacological properties of the KvLQT1/minK channel. The response of KvLQT1/minK to a known blocker XE-991 was tested. Figure 3 (top) shows the IT-plot of the peak amplitude to four concentrations of XE-991 (0.01, 0.1, 1, 10 $\mu$ M). Figure 3 (bottom) shows the corresponding Hill fit. The resulting IC<sub>50</sub> for XE-991 = 0.96 $\pm$ 0.4  $\mu$ M, n=7 (literature value 1-6  $\mu$ M).

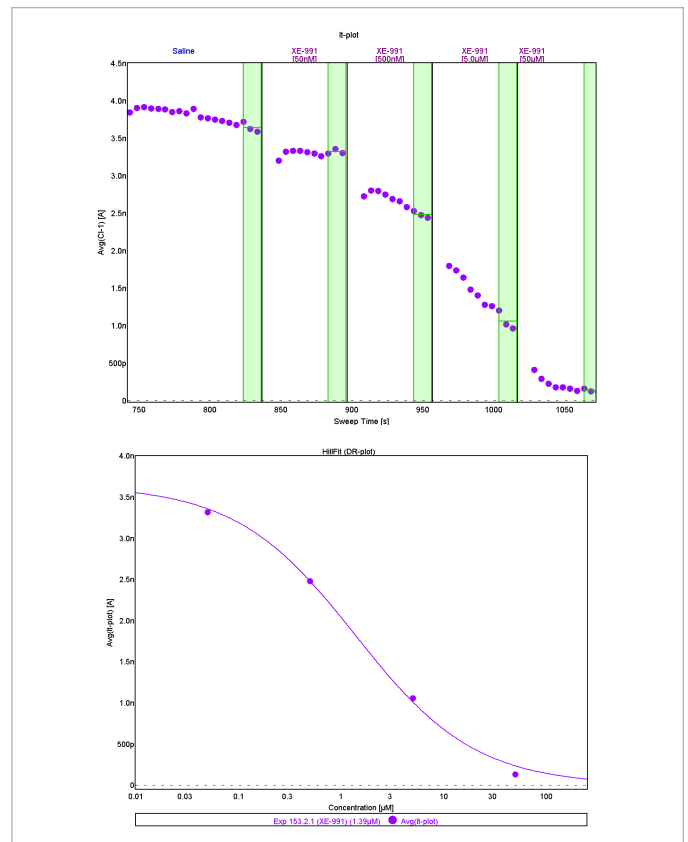


**Fig. 3:** Block of KvLQT1/minK current with XE-991. Top: IT-plot showing the current amplitude in response to four increasing concentrations of XE-991. Bottom: Corresponding Hill fit

Next, the effect on the blocker bepridil was tested on the KvLQT1/minK currents. Figure 4 (top) shows the current-time plot of the peak amplitude in response to four increasing concentrations of bepridil (0.05, 0.5, 5, 50  $\mu$ M). Figure 4 (bottom) shows the corresponding Hill fit. The resulting IC<sub>50</sub> = 8.96 $\pm$ 1.0  $\mu$ M, n=8 (literature value 5.3-10.5  $\mu$ M).

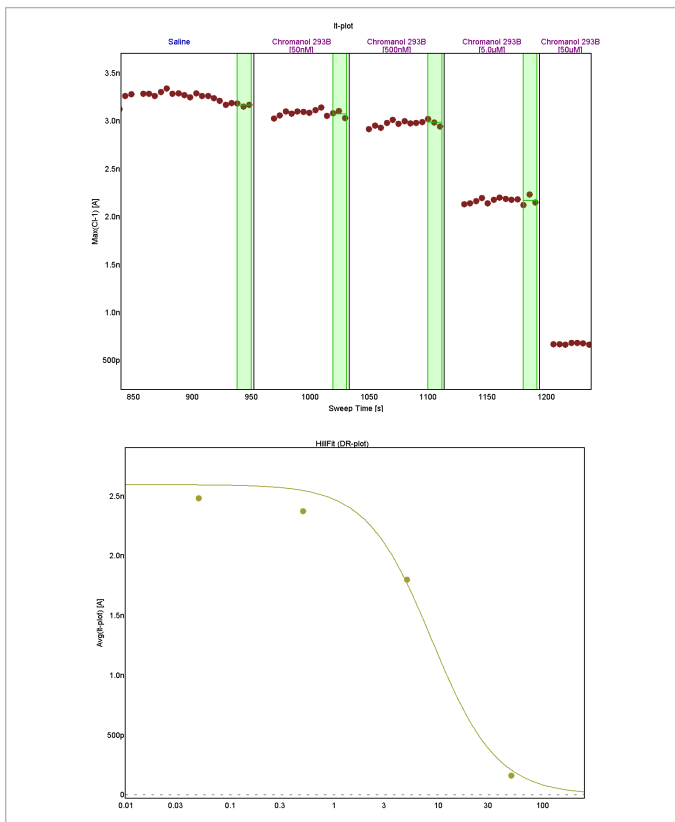


Fig. 4: Block of KvLQT1/minK current with bepridil. Top: IT-plot showing the current amplitude in response to four increasing concentrations of bepridil. Bottom: Corresponding Hill fit.

Furthermore, experiments were performed to evaluate chromanol 293B on KvLQT1/minK currents. Figure 5 (top) shows the current–time plot of the peak amplitude to in relation to four concentrations of chromanol 293B (0.05, 0.5, 5, 50  $\mu\text{M}$ ). Figure 5 (bottom) shows the corresponding Hill fit. The resulting  $\text{IC}_{50}$  for chromanol 293B=  $10.6 \pm 1.1 \mu\text{M}$ ,  $n=13$  (literature value  $10\text{--}12.4 \mu\text{M}$ )

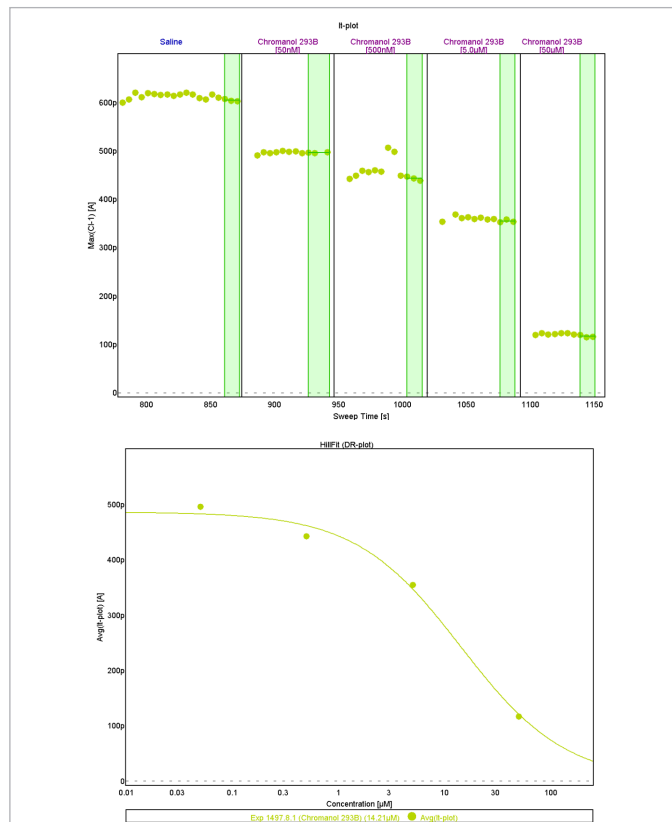


Fig. 5: Block of KvLQT1/minK current with chromanol 293B. Top: IT-plot showing the current amplitude in response to four increasing concentrations of chromanol 293B. Bottom: Corresponding Hill fit.

	XE-991 [ $\mu\text{M}$ ]	Bepridil [ $\mu\text{M}$ ]	Chromanol 293 [ $\mu\text{M}$ ]
$\text{IC}_{50}$	$0.96 \pm 0.4$ , $n=7$	$8.96 \pm 1.0$ , $n=8$	$10.6 \pm 1.1$ , $n=13$

The average peak amplitude was  $2.80 \pm 0.46 \text{ nA}$ ,  $n=28$

QPlate '01065535028240'

Used in job: #1551 - HLO\_KvLQT1/minK\_DR\_1 rerun 1  
Start of use: 2012-01-25 13:30:53

Pos.	Primed	Cell attached	Seal	Whole-cell	R chip [M $\Omega$ ]	R seal [M $\Omega$ ]	R whole-cell [M $\Omega$ ]	WC duration [sec]	Completed exp.
C4	✓	✓	✓	✓	1.69	2826.1	1847.1	544	1
D4	✓	✓	✓	✓	1.68	1828.3	2423.2	127	0
E4	✓	✓	✓	✓	1.70	3004.5	2075.0	544	1
F4	✓	✓	✓	✓	1.72	2120.7	1497.9	79	0
G4	✓	✓	✓	✓	1.69	2240.6	301.5	82	0
H4	✓	✓	✓	✓	1.71	1177.6	548.6	77	0
A5	✓	✓	✓	✓	1.70	1400.5	1339.3	547	1
B5	✓	✓	✓	✓	1.67	1954.2	1537.1	545	1
C5	✓	✓	✓	✓	1.67	2005.3	1724.7	554	0
D5	✓	✓	✓	✓	1.64	1039.1	1053.0	554	0
E5	✓	✓	✓	✓	1.66	1222.3	1376.0	575	0
F5	✓	✓	✓	✓	1.72	1176.8	9.9	0	0
G5	✓	✓	✓	✓	1.72	1952.5	612.0	555	0
H5	✓	✓	✓	✓	1.69	2133.1	1424.5	555	0
A6	✓	✓	✓	✓	1.69	1833.6	1203.3	553	0
B6	✓	✓	✓	✓	1.68	3055.1	1474.8	551	0
C6	✓	✓	✓	✓	1.70	1733.4	1138.0	552	0
D6	✓	✓	✓	✓	1.70	2294.7	1296.1	553	0
E6	✓	✓	✓	✓	1.73	1565.4	1060.1	553	0
F6	✓	✓	✓	✓	1.72	2826.6	1930.6	553	0
G6	✓	✓	✓	✓	1.71	2397.4	1503.8	549	0
H6	✓	✓	✓	✓	1.68	2660.4	1272.3	552	0
Total	47	47	46	45					20
Success rate	98 %	98 %	96 %	94 %					

Fig. 6: QPlate overview showing overall success rate for KvLQT1/minK experiments in single-hole.

## Conclusion

We have demonstrated the functionality of CHO-KvLQT1/minK on QPatch. Biophysical- and pharmacological properties was studied in high resistance whole-cell recordings in IV- and dose-concentration experiments.

We conclude that the CHO-KvLQT1/minK application can be efficiently run on QPatch with high throughput while maintaining high data quality, which match literature values for the given test compounds.

## Methods

### Cells

CHO cells stably expressing KVLQT1/minK were obtained from B'SYS. Cells were cultured and harvested for QPatch experiments as described in the Sophion SOP.

### QPatch

All experiments were performed using the QPatch single-hole and multi-hole technologies and CHO cells expressing the KvLQT1/minK were kept in culture medium in the QStirrer for up to four hours.

### References:

1. S. Y. M. Yeung, I. A. Greenwood 2005. Electrophysiological and functional effects of the KCNQ channel blocker XE991 on murine portal vein smooth muscle cells. *Br J Pharmacol.* 146 (4): 585-595
2. A. R. Mackie, K. L. Byron 2008. Cardiovascular KCNQ (K<sub>v</sub>7) potassium channels: Physiological regulators and new therapeutic intervention. *Mol Pharmacol fast forward.* 74 (5): 1171-1179